EFFICIENT CRITICAL EXCITATION METHOD USING IMPULSE INPUT FOR PULSE-LIKE AND LONG-DURATION GROUND MOTIONS

K. Kojima[(1)], I. Takewaki[(2)]

[(1)] *Assistant Professor, Faculty of Design and Architecture, Kyoto Institute of Technology, kojima61@kit.ac.jp*
[(2)] *Professor, Department of Architecture and Architectural Engineering, Kyoto University, takewaki@archi.kyoto-u.ac.jp*
…

Abstract

Pulse-like earthquake ground motions have been observed near earthquake source faults during large-scale earthquakes, e.g. the Northridge earthquake in 1994, the Hyogo-ken Nanbu earthquake in 1995, the Chi-Chi (Taiwan) earthquake in 1999 and the Kumamoto earthquake in 2016. Structural damages have been reported after such inland earthquake events. On the other hand, long-period and long-duration ground motions have been observed during large earthquake events such as the Niigata-ken Chuetsu earthquake in 2004 and the Tohoku earthquake in 2011, and some high-rise buildings were in resonance with these ground motions.

In this paper, the double and multiple impulses are introduced for substituting the pulse-like ground motions, which can be represented by a few series of sinusoidal wavelets, and the long-duration ground motions, which can be represented by harmonic waves [1, 2]. Then the critical and non-critical elastic-plastic responses subjected to the double impulse and the multiple impulse are derived in closed form. The critical responses represent the resonance, and the proposed method enables an explicit evaluation of the resonant response of inelastic systems that requires complex procedures in conventional methods [1, 2]. The response to the impulse input can be expressed by the instantaneous increase of the velocity of mass, and the system exhibits free vibration after each impulse. The closed-form solutions for the critical elastic-plastic responses under the double and multiple impulses can be derived by finding the critical timing and using the energy balance law, where the kinetic energy imparted at the impulse acting point is equal to the sum of the elastic strain energy and the energy dissipation by the plastic deformation. The critical timing of the second impulse of the double impulse input is found to be the zero-restoring force timing after the first impulse for the inelastic single-degree-of-freedom system. Similarly, the critical timing of each impulse of the multiple impulse input is found to be the zero-restoring force timing after the previous impulse. It is noted that the elastic strain energy is zero at the critical impulse timing. On the other hand, the inelastic response under the non-critical double and multiple impulses can also be derived in closed form by using the energy balance law and the free-vibration response after the previous impulse.

It is further shown that an approximate elastic-plastic response spectrum for a pulse-like near-fault ground motion can be obtained analytically, i.e. without time-history response analysis. Although strength-modified iterative calculation without reliable convergence confirmation for a specified ductility factor is necessary to obtain the elastic-plastic response spectrum for actually recorded ground motions in the conventional procedure, the proposed closed-form expression provides an analytical and efficient evaluation for the elastic-plastic response spectrum for the characterized pulse-like ground motion. In detail, the proposed critical and non-critical inelastic response expressions enable the derivation of closed-form natural periods for a specific ductility factor with respect to strength parameter. Then the natural periods for various strength parameters under a constant ductility factor lead to the plot of the elastic-plastic response spectrum without unreliable iterative procedures. The validity of the elastic-plastic response spectrum for the double impulse representing pulse-like ground motions is investigated through the comparison with the elastic-plastic response spectra for actual recorded pulse-like ground motions.

Keywords: Critical Response; Elastic-plastic Response; Near-fault Ground Motion; Double Impulse; Multiple Impulse

1. Introduction

Pulse-like earthquake ground motions have been observed near earthquake source faults during large-scale earthquakes including the Northridge earthquake in 1994, the Hyogo-ken Nanbu earthquake in 1995, the Chi-Chi (Taiwan) earthquake in 1999 and the Kumamoto earthquake in 2016. Structural damages have been reported after such inland earthquake events. Near-fault pulse-like ground motions can be roughly classified into the fling-step and forward-directivity inputs, and the main part of these two pulse-like inputs can be expressed by a few wavelet combinations [3]. In the recent papers, the fling-step input can be represented by a one-cycle sinusoidal wave and the forward-directivity input can be modelled by three series of sinusoidal wavelets or Ricker wavelet [3, 4]. Furthermore, it should be noted that these ground motions cause large plastic deformations of building structures during large inland earthquake events, and the effects of pulse-like inputs on building structures have been studied recently [3, 4]. Alternatively, long-period and long-duration ground motions have been recorded during earthquake events with large magnitude such as the Niigata-ken Chuetsu earthquake in 2004 and the Tohoku earthquake in 2011 [5]. In the 1970s, these long-period and long-duration ground motions were not expected in the structural design of base-isolation buildings and super high-rise buildings, whose natural periods are longer than 4.0[sec], and such long-period building structures may be damaged or collapse due to resonance with such long-period and long-duration ground motions. Therefore, it is necessary to investigate the resonant phenomenon of long-period buildings to such ground motions. In previous works, the main part of these long-duration ground motions can be modeled by multi-cycle sinusoidal waves, and the resonant phenomenon and elastic-plastic responses of the building structures have been checked by using such equivalent long-duration ground motions [6].

The resonance and critical responses of inelastic structural systems subjected to pulse-like or long-duration inputs are important in the earthquake-resistant design, and a great number of theoretical investigations on inelastic responses under earthquake ground motions have been accumulated. Caughey derived a resonance curve of a single-degree-of-freedom (SDOF) bilinear hysteretic system. In this study, the resonance curve can be calculated by the equivalent linearization method based on a least-squares approximation [7]. On the other hand, Iwan derived the exact solution for the steady-state response of an undamped SDOF bilinear hysteretic system and an approximate solution for that of an undamped two DOF bilinear hysteretic system subjected to the harmonic wave [8]. However, these two methods are too complicated to calculate the resonant response of elastic-plastic structures, because the resonant responses of the elastic-plastic structures have to be calculated for a specific input level, e.g. the acceleration amplitude and the velocity amplitude, by changing the input frequency.

To overcome such difficulty, Kojima and Takewaki have introduced double, triple and multiple impulse inputs substituting the fling-step input, forward-directivity input and long-duration ground motion [1, 2, 9-11]. The critical elastic-plastic responses, which represent the resonant responses, subjected to these impulse inputs are derived in closed form, and the proposed method enables an explicit evaluation of the resonant responses of inelastic systems that requires complex procedures in conventional methods [1, 2, 9-11]. The closed-form solutions for the critical inelastic responses subjected to such impulse train inputs can be derived by finding the critical timing and using the energy balance law. The response to such impulse inputs can be represented by the free vibration with the instantaneous increase of velocity of mass, and the kinetic energy imparted at the impulse acting point is equal to the sum of the elastic strain energy and the energy dissipation by the plastic deformation at the point where the system reaches the maximum displacement. The critical timing of the subsequent impulse of the impulse inputs is found to be the timing when the restoring force becomes zero after the previous impulse for the inelastic SDOF system. It is noted that the elastic strain energy is zero at the critical timing.

In this paper, the double and multiple impulse inputs are introduced for substituting the pulse-like ground motions, which can be represented by a few combinations of sinusoidal wavelets, and the long-duration ground motions, which can be expressed by harmonic waves [1, 2, 9-11]. Then the critical and non-critical inelastic responses subjected to the double and multiple impulse inputs are obtained in closed form. The inelastic responses to the non-critical double and multiple impulses can also be derived in closed form by using the energy balance law and the free-vibration response after the previous impulse. It is further shown that an approximate elastic-plastic response spectrum for a pulse-like near-fault input can be obtained analytically. Although strength-modified iterative calculation without reliable convergence confirmation for a specified ductility factor is necessary to calculate the elastic-plastic response spectrum for actually recorded ground motions, the proposed closed-form expression provides an analytical and efficient evaluation for the inelastic response spectrum for the characterized pulse-like ground motion. The validity of the proposed response spectrum for the double impulse representing pulse-like ground motions is checked through the comparison with the inelastic response spectra for actual recorded pulse-like inputs.

2. Double and multiple impulse inputs

2.1 Double impulse input

The acceleration of the fling-step input, which is the fault-parallel component of near-fault ground motions, can be characterized by a one-cycle sine wave as shown in Fig.1(a), and the double impulse input has been introduced to substitute the fling-step inputs [1, 9].

A ground acceleration $\ddot{u}_g(t)$ of the double impulse as shown in Fig.1(a) is expressed by

$$\ddot{u}_g(t) = V\delta(t) - V\delta(t - t_0) \tag{1}$$

where V denotes the velocity provided by the first and second impulses (the velocity amplitude), t_0 represents the time interval between two impulses and $\delta(t)$ is the Dirac delta function. The comparison of the waveform of the double impulse input with a one-cycle sine wave is shown in Fig.1(a). A ground acceleration $\ddot{u}_g^{SW}(t)$ of the one-cycle sine wave is expressed by

$$\ddot{u}_g^{SW}(t) = A_p \sin(\omega_p t) \qquad (0 \le t \le T_p = 2t_0) \tag{2}$$

where A_p denotes the acceleration amplitude of the sine wave and ω_p ($=2\pi/T_p$) denotes of the input circular frequency. The velocity amplitude V of the double impulse corresponds to the maximum velocity $V_p = 2A_p/\omega_p$ of the corresponding one-cycle sine wave, and the time interval t_0 is equal to a half of the period of the sine wave. To compare the inelastic response to the double impulse and that to the sine wave, the velocity amplitude V of the double impulse has to be adjusted to that V_p of the sine wave. In this paper, the velocity amplitudes of the two inputs are adjusted to make the maximum Fourier amplitude of the double impulse equal to that of the sine wave [9]. The ratio of V_p to V is 1.2222 based on the above adjustment method and the validity of this method has been investigated in the previous paper [9].

2.2 Multiple impulse input

The long-duration ground motions are modelled by the multiple impulse input as shown in Fig.1(b) [2, 10]. A ground acceleration $\ddot{u}_g(t)$ of the multiple impulse input with the equal time interval is represented by

$$\ddot{u}_g(t) = 0.5V\delta(t) - V\delta(t-t_0) + V\delta(t-2t_0) - V\delta(t-3t_0) + \cdots + (-1)^N V\delta\{t-(N-1)t_0\} + 0.5V\delta(t-Nt_0) \tag{3}$$

where V denotes the velocity provided by each impulse (the velocity amplitude), t_0 denotes the time interval between two consecutive impulses and N is the number of impulses (N is an even number). The comparison of acceleration, velocity and displacement of the multiple impulse input with the sine wave is shown in Fig.1(b). A ground acceleration $\ddot{u}_g^{SW}(t)$ of the multi-cycle sine wave is expressed by

$$\ddot{u}_g^{SW}(t) = \begin{cases} 0.5A_l \sin(\omega_l t) & (0 \le t < 0.5T_l, 0.5NT_l < t \le 0.5(NT_l)) \\ A_l \sin(\omega_l t) & (0.5T_l \le t \le 0.5NT_l) \end{cases} \tag{4}$$

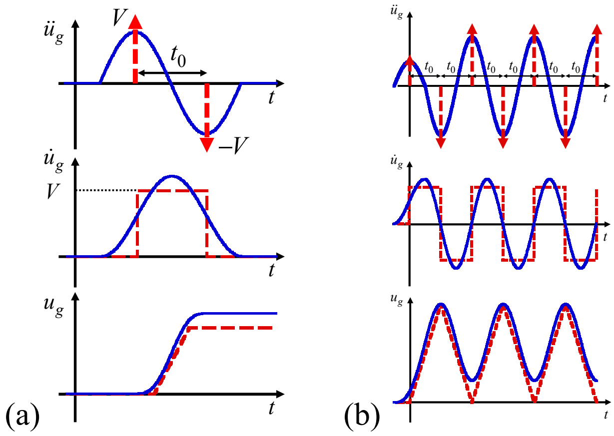

Fig. 1 – Simple ground motion models by impulse train inputs: (a) Pulse-like ground motion and double impulse [1,9,11], (b) Long-duration input and multiple impulse input [2,10]

where A_1 represents the acceleration amplitude of the sine wave and ω_1 ($=2\pi/T_1$) denotes the input circular frequency. The velocity amplitude V of the multiple impulse input corresponds to the that $V_1 = 2A_1/\omega_1$ of the sine wave and the time interval t_0 is equal to a half of the period of the sine wave. The velocity amplitude of the double impulse is also adjusted to that of the sine wave to compare the elastic-plastic responses. In this paper, $V_1/V = 2/\pi$ is adopted [10]. The ratio $V_1/V = 2/\pi$ has also been derived based on the equivalence of the maximum Fourier amplitude [10].

3. Inelastic response to double impulse

3.1 Critical response of elastic-perfectly plastic SDOF system subjected to double impulse

Consider an undamped SDOF elastic-perfectly plastic system as shown in Fig.2(a). The mass, stiffness, natural circular frequency and natural period of the SDOF system are denoted by m, k, $\omega_1 = \sqrt{k/m}$ and T_1 ($=2\pi/\omega_1$), respectively. Let u and f denote the displacement of the mass relative to the ground and the restoring force (see Fig.2(a)). u is equal to the deformation of the system. The yield deformation and yield force are denoted by d_y and f_y ($=kd_y$), respectively, as shown in Fig.2(b).

A closed-form expression has been derived for the inelastic response of the undamped elastic-perfectly plastic SDOF system subjected to the critical double impulse [1]. The maximum inelastic responses of the undamped system under the critical double impulse input can be obtained by an energy approach without solving directly the equation of motion. Furthermore, the critical timing of the second impulse can be found as the time when the restoring force becomes zero in the unloading range after the first impulse, and the maximum deformation after the second impulse is maximized by using such critical timing. The critical time interval t_0^c can also be obtained analytically for the increasing velocity amplitude of the double impulse input. t_0^c corresponds to a half of the inelastic resonant period of the sine wave.

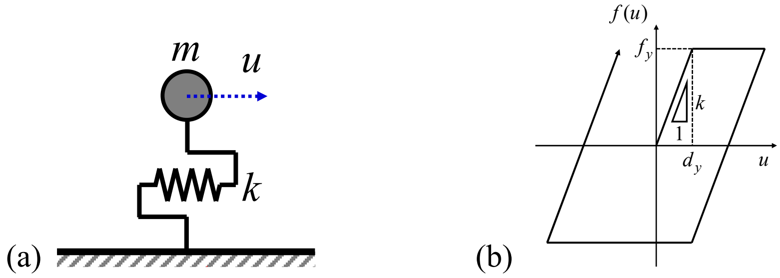

Fig. 2 – Undamped elastic-perfectly plastic SDOF system: (a) SDOF system, (b) Elastic-perfectly plastic restoring force-deformation relation [9]

Fig.3 shows the restoring force-deformation relations to the critical double impulse. $u_{\max 1}$ and $u_{\max 2}$ in Fig.3 represent the maximum deformation after the first and second impulses. The inelastic responses under the critical double impulse can be divided into three cases, depending on the velocity amplitude and yielding stage. CASE 1 is the elastic case even after the second impulse, CASE 2 is the case where the system goes into the plastic range just after the second impulse and CASE 3 is the case where the system exceeds yield deformation after the first impulse. Fig.3(a)-(c) show a schematic diagram of CASEs 1-3. $V_y = \omega_1 d_y$ is introduced to normalize the velocity amplitude V. The maximum deformation of the undamped SDOF system subjected to the single impulse with V_y just reaches the yield deformation d_y. In this paper, the ratio V/V_y is used to express the input velocity level. The normalized maximum deformation $u_{\max 1}/d_y$ and $u_{\max 2}/d_y$ after the first and second impulses in CASEs 1-3 can be obtained by

$$\frac{u_{\max 1}}{d_y} = \begin{cases} V/V_y & (0 \le V/V_y < 1.0 : \text{CASE } 1,2) \\ 0.5\{1+(V/V_y)^2\} & (1.0 \le V/V_y : \text{CASE } 3) \end{cases} \tag{5}$$

$$\frac{u_{\max 2}}{d_y} = \begin{cases} 2V/V_y & (0 \le V/V_y < 0.5 : \text{CASE1}) \\ 0.5\{1+(2V/V_y)^2\} & (0.5 \le V/V_y < 1.0 : \text{CASE2}) \\ 1.5+(V/V_y) & (1.0 \le V/V_y : \text{CASE3}) \end{cases} \tag{6}$$

The critical time interval t_0^{c} in CASEs 1-3 can also be obtained by the following equations.

$$\frac{t_0^{\mathrm{c}}}{T_1} = \begin{cases} 0.5 & (0 \le V/V_y < 1.0 : \text{CASE } 1,2) \\ \{\arcsin(V_y/V) + \sqrt{(V/V_y)^2 - 1}\}/(2\pi) + 0.25 & (1.0 \le V/V_y : \text{CASE } 3) \end{cases} \tag{7}$$

Fig.4 shows the normalized maximum inelastic response $u_{\max}/d_y = \max(u_{\max 1}, u_{\max 2})/d_y$ to the critical double impulse input with respect to the input level V/V_y. Fig.5 illustrates the critical time interval t_0^{c} normalized by the natural period T_1 with respect to the input level V/V_y.

3.2 Non-critical response of elastic-perfectly plastic SDOF system subjected to double impulse

A closed-form expression is derived for the response of the undamped elastic-perfectly plastic SDOF system subjected to the non-critical double impulse [11]. The inelastic response to the non-critical double impulse can also be derived in closed form by using the energy balance law and the expression on free vibration after the first impulse.

First, consider the input level range $0 \le V/V_y < 0.5$, where the critical response is in the elastic range. The maximum deformation $u_{\max 1}/d_y$ and $u_{\max 2}/d_y$ after the first and second impulse can be obtained by

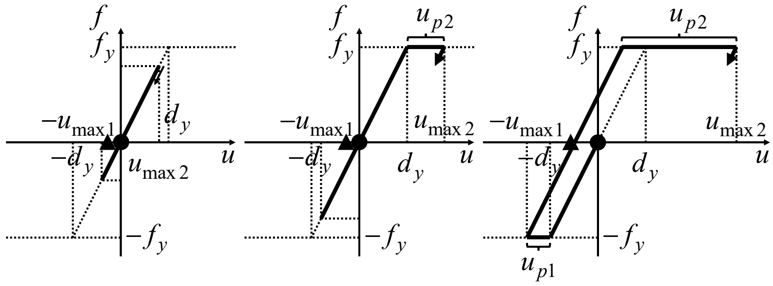

Fig. 3 – Maximum inelastic deformation of undamped SDOF system under critical double impulse input: (a) CASE 1, (b) CASE 2, (c) CASE 3 (●: first impulse, ▲: second impulse) [9]

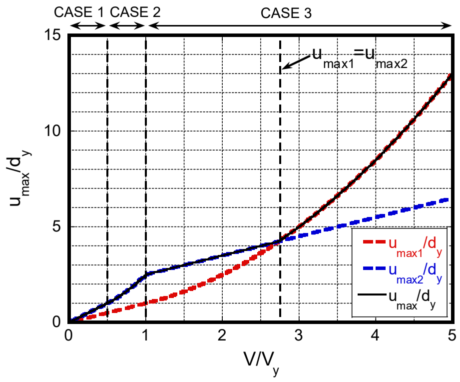

Fig. 4 – Maximum response u_{max}/d_y to critical double impulse with V/V_y [1]

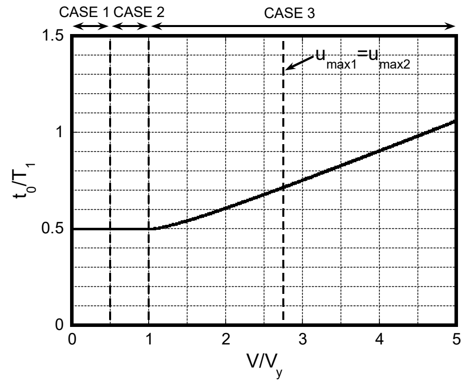

Fig. 5 – Critical time interval t_0^c/T_1 with respect to input level V/V_y [1]

$$u_{\max 2} / d_y = (V / V_y)\sqrt{2 - 2\cos(2\pi t_0 / T_1)} \tag{9}$$

Second, consider the input level range 0.5≤ V/V_y<1.0, where the critical response goes into the plastic range just after the second impulse. Since $u_{\max1}$ does not exceed d_y, $u_{\max1}$ in the input level range 0.5≤ V/V_y <1.0 can be also obtained from Eq. (8). When $u_{\max2}$ is in the elastic range, $u_{\max2}/d_y$ in this input level can also be derived by Eq. (9). When $u_{\max2} > d_y$, $u_{\max2}/d_y$ can be obtained by

$$u_{\max 2} / d_y = 0.5[1 + (V / V_y)^2 \{2 - 2\cos(2\pi t_0 / T_1)\}] \qquad (\cos(2\pi t_0 / T_1) \le 1 - 0.5(V_y / V)^2) \tag{10}$$

Finally, consider the input level range 1.0 ≤ V/V_y, where the critical response is in the plastic range after the first impulse. Figure 6 shows a schematic diagram of the inelastic response under the non-critical double impulse. $u_{\max1}/d_y$ can be obtained by

$$\frac{u_{\max 1}}{d_y} = \begin{cases} (V / V_y)\sin(2\pi t_0 / T_1) & (t_0 / T_1 < t_{\mathrm{OA}} / T_1) \\ -[2\pi^2 \{(t_0 - t_{\mathrm{OA}}) / T_1\}^2 - 2\pi\{\sqrt{(V / V_y)^2 - 1}\}\{(t_0 - t_{\mathrm{OA}}) / T_1\} - 1] & (t_{\mathrm{OA}} / T_1 \le t_0 / T_1 < t_{\mathrm{OB}}) \\ 0.5\{1 + (V / V_y)^2\} & (t_{\mathrm{OB}} / T_1 \le t_0 / T_1) \end{cases} \tag{11}$$

where t_{OA}= arcsin(V_y/V)/(2π) and t_{AB}= $\sqrt{(V/V_y)^2 - 1}\,/(2\pi)$ are the time interval between point O and point A and that between point A and point B in Fig.6, and t_{OB} = t_{OA} + t_{AB}. When $t_0 < t_{\mathrm{OA}}$ as shown in Fig.6(a), $u_{\max2}/d_y$ in this input level can also be obtained by Eqs. (9) and (10). When $t_{\mathrm{OA}} \le t_0 < t_{\mathrm{OB}}$ as shown in Fig.6(b), the maximum response after the second impulse is in the plastic range and $u_{\max2}/d_y$ can be obtained as follows.

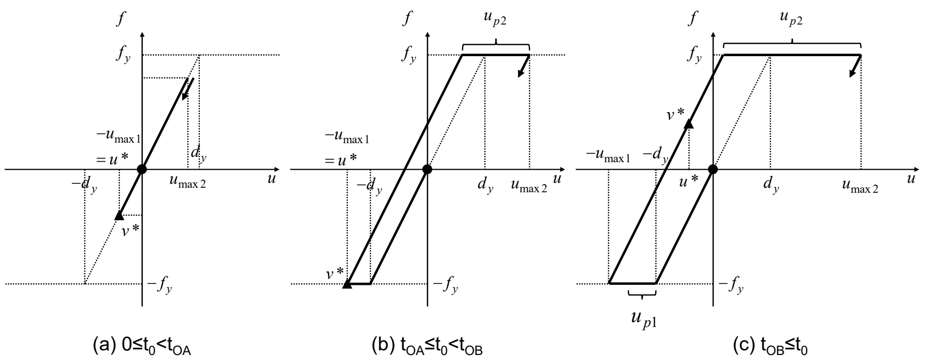

Fig. 6 – Maximum inelastic deformation under non-critical double impulse input for input level range $1.0 \le V / V_y$: (a) $t_0 < t_{\mathrm{OA}}$, (b) $t_{\mathrm{OA}} \le t_0 < t_{\mathrm{OB}}$, (c) $t_{\mathrm{OB}} \le t_0$ (●: first impulse, ▲: second impulse)

$$u_{\max 2}/d_y = \{(2\pi)(t_0 - t_{OA})/T_1\}^2 + \{(V/V_y) - 2\sqrt{(V/V_y)^2 - 1}\}\{(2\pi)(t_0 - t_{OA})/T_1\} + 0.5\{(V/V_y) - \sqrt{(V/V_y)^2 - 1}\}^2 + 1 \quad (12)$$

When $t_{OB} \leq t_0$ as shown in Fig.6(c) and the maximum response after the second impulse is in the plastic range, u_{max2}/d_y can be expressed by

$$u_{\max 2}/d_y = 1.5 + (V/V_y)\sin\{(2\pi)(t_0 - t_{OB})/T_1\} \quad (13)$$

When $t_{OB} \leq t_0$ and the maximum response after the second is in the elastic range, u_{max2}/d_y can be obtained by

$$u_{\max 2}/d_y = \sqrt{1 + (V/V_y)^2 + 2(V/V_y)\sin\{2\pi(t_0 - t_{OB})/T_1\}} - 0.5\{(V/V_y)^2 - 1\} \quad (14)$$

Fig.7 shows the maximum deformation u_{max}/d_y under the non-critical double impulse with respect to the time interval t_0/T_1.

4. Steady-state inelastic response to multiple impulse

4.1 Critical steady-state response of elastic-perfectly plastic SDOF system under multiple impulse

The steady-state inelastic response has been derived analytically for an undamped SDOF elastic-perfectly plastic system subjected to the critical multiple impulse input [2]. The plastic deformation to the critical multiple impulse input can also be obtained by using an energy approach without solving directly the differential equation (equation of motion). The critical timing of each impulse can be characterized as the time when the restoring force attains zero in the unloading process after the previous impulse, and the plastic deformation becomes maximum to such critical input. The critical time interval t_0^c corresponds to a half of the resonant period of the sine wave to the inelastic system and t_0^c can be obtained as a function of V/V_y.

A schematic diagram of the steady state inelastic responses to the critical multiple impulse input is shown in Fig.8. u_p in Fig.8 denotes the plastic deformation in steady state. The normalized plastic deformation u_p/d_y can be obtained by

$$u_p/d_y = 0.5\{2(V/V_y) + (V/V_y)^2\} \quad (15)$$

The critical timing t_0^c of the multiple impulse input can also be expressed by

$$t_0^c/T_1 = [\arcsin\{1 + (V/V_y)\}^{-1} + \sqrt{(V/V_y)^2 + 2(V/V_y)}]/(2\pi) + 0.25 \quad (16)$$

Figs. 9 and 10 show the normalized plastic deformation u_p/d_y and the critical time interval t_0^c/T_1 with respect to V/V_y for the multiple impulse input.

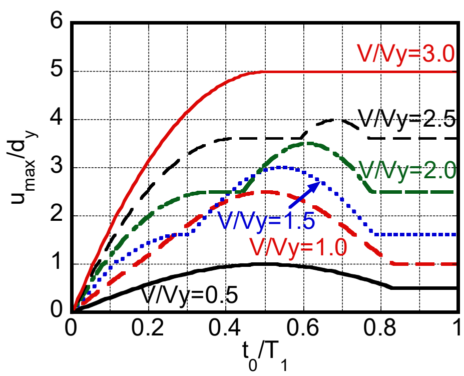

Fig. 7 – Maximum deformation u_{max}/d_y to non-critical double impulse with t_0/T_1 for varied V/V_y

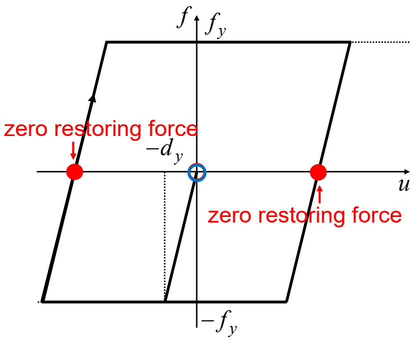

Fig. 8 – Steady-state response to critical multiple impulse (●: acting points of impulses) [2]

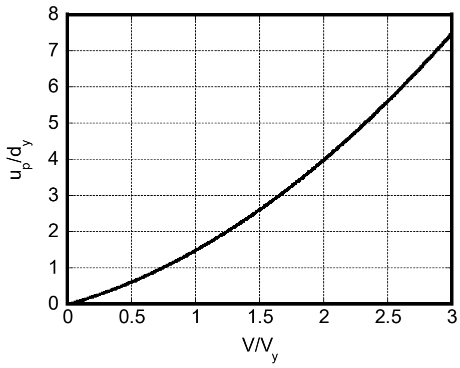

Fig. 9 – Plastic deformation u_p/d_y to critical multiple impulse with varied V/V_y [2]

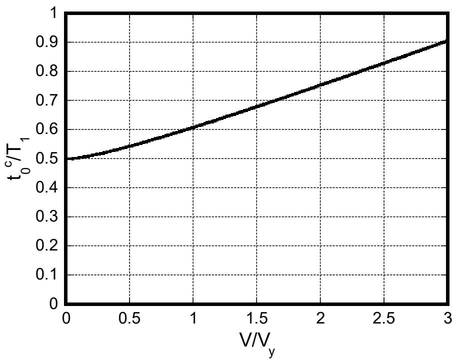

Fig. 10 – Critical time interval t_0^c/T_1 with respect to input level V/V_y [2]

4.2 Non-critical response of elastic-perfectly plastic SDOF system under multiple impulse

The plastic deformation in steady state to a non-critical multiple impulse input is derived. The steady state is assumed where the impulse acting point converges to the two points as shown in Fig.11. t^* is defined as the time interval between point E' and F' in Fig.11. d^* and v^* in Fig.11 can be obtained as follows.

$$d^* = d_y \cos(\omega_1 t^*) \,,\, v^* = V_y \sin(\omega_1 t^*) \tag{17), (18}$$

By using d^*, v^* and solving the differential equation (equation of motion), the time interval $t_{\mathrm{F'D}}$ between point F' and point D and that t_{DE} between point D and point E can be derived in terms of t^*.

$$t_{\mathrm{F'D}} / T_1 = \{(\pi/2) - \phi + \arcsin[(V/V_y)^2 + 2(V/V_y)\sin(\omega_1 t^*) + 1]^{-0.5}\} / (2\pi) \tag{19}$$

$$t_{\mathrm{DE}} / T_1 = \sqrt{(V/V_y)^2 + 2(V/V_y)\sin(\omega_1 t^*)} \,/\, (2\pi) \tag{20}$$

where $\phi = \arctan[\{\sin(\omega_1 t^*)+(V/V_y)\}/\cos(\omega_1 t^*)]$. Therefore, the time interval t_0 of the non-critical multiple impulse input can be obtained by using t^* as follows.

$$\begin{aligned} t_0 / T_1 &= (t^*/T_1) + (t_{\mathrm{F'D}}/T_1) + (t_{\mathrm{DE}}/T_1) \\ &= (t^*/T_1) + \{(\pi/2) - \phi + \arcsin[(V/V_y)^2 + 2(V/V_y)\sin(\omega_1 t^*) + 1]^{-0.5}\} / (2\pi) \\ &\quad + \{\sqrt{(V/V_y)^2 + 2(V/V_y)\sin(\omega_1 t^*)}\} / (2\pi) \end{aligned} \tag{21}$$

On the other hand, the plastic deformation to the non-critical multiple impulse input can be obtained by an energy balance law. The energy balance law between point F' and point E is expressed by

$$0.5m(v^* + V)^2 + 0.5kd^{*2} = 0.5kd_y^{\,2} + f_y u_p \tag{22}$$

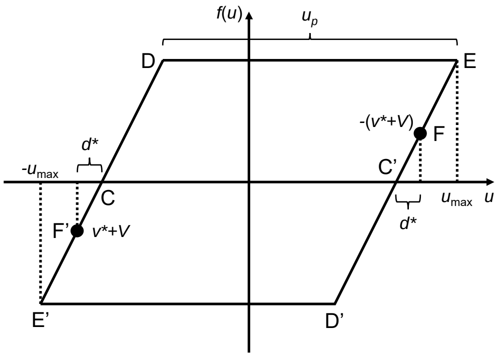

Fig. 11 – Restoring force-deformation relation in steady state to non-critical multiple impulse input

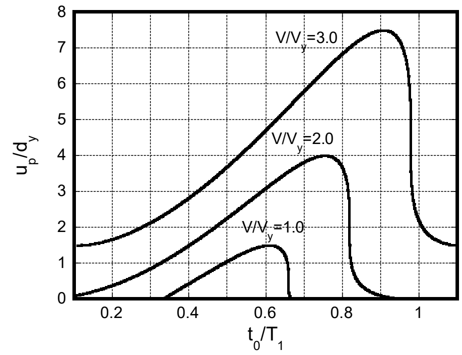

Fig. 12 – Plastic deformation u_p/d_y to non-critical multiple impulse with t_0/T_1 for specific V/V_y

From Eq. (22), the plastic deformation u_p/d_y can be derived in terms of t^* by

$$u_p / d_y = (V / V_y)\sin(\omega_1 t^*) + 0.5(V / V_y)^2 \tag{23}$$

Although it is difficult to calculate u_p/d_y directly from the time interval t_0/T_1, the relation between u_p/d_y and t_0/T_1 can be obtained from Eqs. (21) and (23) by using t^*. The relation between the plastic deformation u_p/d_y to the non-critical multiple impulse and t_0/T_1 can be obtained by Eqs. (21) and (23) as shown in Fig.12.

5. Elastic-plastic response spectrum for double impulse input

An elastic-plastic response spectrum for the double impulse input is derived by using the critical and non-critical double impulse. The elastic-plastic response spectrum for the double impulse can be obtained by using the relation between the ductility factor and the natural period normalized by the time interval of the double impulse. In this paper, the ductility factor is equal to the maximum deformation normalized by the yield deformation. Fig.13 shows the flowchart for deriving the elastic-plastic response spectrum for the double impulse. First, the minimum input level $(V/V_y)_{\min}$ for a specific ductility factor μ is obtained by the critical elastic-plastic responses derived from Eqs. (5) and (6). The minimum input level $(V/V_y)_{\min}$ can be classified into $(V/V_y)_{\min 1}$, $(V/V_y)_{\min 2}$ and $(V/V_y)_{\min 3}$ depending on the ductility factor μ. Then the relation between (V/V_y) and (t_0/T_1) is obtained from the non-critical inelastic responses, which were explained in section 3.2. Finally, the elastic-plastic response can be obtained from the relation between (V/V_y) and (t_0/T_1). It is noted that the velocity amplitude V and the time interval t_0 of the double impulse equivalent to the pulse-like ground motions are necessary to obtain the elastic-plastic spectrum. These two parameters represent the pulse characteristics of the ground motions.

The maximum deformation under the double impulse can be classified into the maximum deformation $u_{\max 1}$ just after the first impulse and the maximum deformation $u_{\max 2}$ after the second impulse. First, the relation between the ductility factor μ $(=u_{\max 1}/d_y)$ and the normalized natural period t_0/T_1 is derived. From Eq. (11), μ $(=u_{\max 1}/d_y)$ and $\tau = (t_0 - t_{OA})(2\pi/T_1)$, the following equation can be obtained.

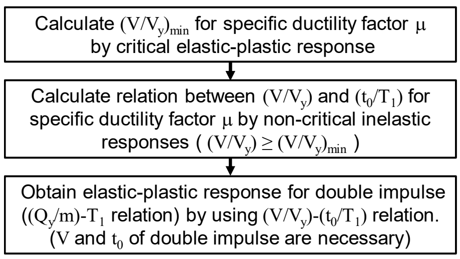

Fig. 13 – Flowchart of derivation of elastic-plastic response spectrum for double impulse

$$\mu = -0.5\tau^2 + \sqrt{(V/V_y)^2 - 1}\tau + 1 \tag{24}$$

From Eq. (24), $\tau = (t_0 - t_{OA})(2\pi/T_1)$ can be derived as follows.

$$\tau = \sqrt{(V/V_y)^2 - 1} - \sqrt{(V/V_y)^2 - 2\mu + 1} \tag{25}$$

By using Eq. (25) and t_{OA}= arcsin(V_y/V)/(2π), t_0/T_1 can be obtained as the function of μ and (V/V_y).

$$t_0 / T_1 = \left\{ \arcsin(V_y / V) + \sqrt{(V/V_y)^2 - 1} - \sqrt{(V/V_y)^2 - 2\mu + 1} \right\} / (2\pi) \tag{26}$$

where $1.0 \leq V/V_y$. Furthermore, the minimum input level $(V/V_y)_{\min1}$ for a specific ductility factor μ can be obtained from the maximum response $u_{\max1}$ after the first impulse as follows.

$$(V/V_y)_{\min 1} = \sqrt{2\mu - 1} \tag{27}$$

In addition, the input level for the specific μ is $(V/V_y)_{\min1}$ regardless of t_0/T_1 when $t_0 < t_{OA}$.

Secondly, the relation between μ (=$u_{\max2}/d_y$) and t_0/T_1 is derived for the maximum deformation $u_{\max2}$ after the second impulse. By using Eq. (13), μ (=$u_{\max2}/d_y$) and $\tau = (t_0 - t_{OB})(2\pi/T_1)$, the following equation can be derived when the ductility factor μ exceeds 2.5 (CASE 3).

$$\mu = 1.5 + (V/V_y)\sin\tau \tag{28}$$

From Eq. (28), τ can be derived as follows.

$$\tau = \arcsin\{(\mu - 1.5)/(V/V_y)^2\} \tag{29}$$

Eq. (29) provides t_0/T_1 as

$$t_0 / T_1 = [\arcsin(V_y / V) + \sqrt{(V/V_y)^2 - 1} + \arcsin\{(\mu - 1.5)/(V/V_y)^2\}]/(2\pi) \tag{30}$$

where $1.0 \leq V/V_y$ and $\mu \geq 2.5$. From $u_{\max2}/d_y$=1.5+(V/V_y) in CASE 3, the minimum input level $(V/V_y)_{\min2}$ for a specific ductility factor μ can be obtained as follows.

$$(V/V_y)_{\min 2} = \mu - 1.5 \tag{31}$$

Finally, the relation between μ (=$u_{\max2}/d_y$) and t_0/T_1 is derived for $u_{\max2}$ in the input level range $0.5 \leq V/V_y < 1.0$ (CASE 2). When $1.0 \leq \mu < 2.5$, the following equation can be derived from Eq. (10) and $\mu = u_{\max2}/d_y$.

$$\mu = 0.5 + 0.5(V/V_y)^2[2 - 2\cos\{t_0(2\pi/T_1)\}] \tag{32}$$

From Eq. (32), t_0/T_1 can be obtained by

$$t_0 / T_1 = \arccos[1 - 0.5\{(2\mu - 1)/(V/V_y)^2\}]/(2\pi) \tag{33}$$

where $0.5 \leq V/V_y < 1.0$. From $u_{\max2}/d_y = 0.5\{1+(2V/V_y)^2\}$ in CASE 2, the minimum input level $(V/V_y)_{\min3}$ for a specific ductility factor μ can be obtained as follows.

$$(V/V_y)_{\min 3} = 0.5\sqrt{2\mu - 1} \tag{34}$$

The relation between the input level (V/V_y) and the normalized time interval (t_0/T_1) for a specific ductility factor μ provides the relation between the yield force (strength) Q_y/m normalized by mass and the natural period T_1. From (V/V_y) and (t_0/T_1), Q_y/m can be obtained as follows.

$$(Q_y / m) = kd_y / m = \omega_1^2 d_y = (2\pi / T_1)V_y = 2\pi(t_0 / T_1)(V/V_y)^{-1}(V/t_0) \tag{35}$$

The elastic-plastic response spectrum can be obtained by using Eq. (35) for the double impulse as a representative of the pulse-like ground motions in terms of the velocity amplitude V and the time interval t_0 corresponding to the pulse period.

Fig.14 shows the relation between (V/V_y) and (t_0/T_1) for various ductility factors μ =3.0-6.0. Fig.15(a) shows the elastic-plastic response spectrum for the double impulse with V = 1.64 [m/sec] and t_0 = 0.4 [sec]. These two parameters are the parameters of the double impulse modelling Rinaldi Station FN component during the Northridge earthquake in 1994. Fig.15(b) shows the elastic-plastic response spectrum for Rinaldi Station FN component. The ground acceleration of Rinaldi Station FN from 0 sec to 3.3 [sec] is used to consider the response to the principal part with strong pulse characteristics. The elastic-plastic response spectrum for the double impulse with V = 1.64 [m/sec] and t_0 = 0.4 [sec] corresponds to that for Rinaldi station FN component within reasonable accuracy.

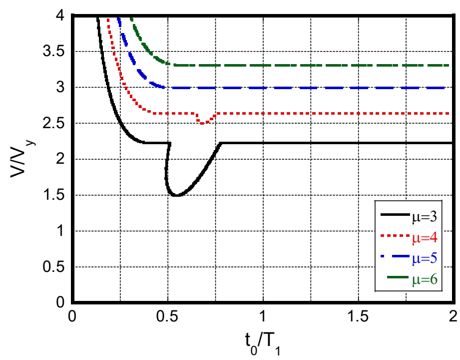

Fig. 14 – (V/V_y) - (t_0/T_1) relation for specified ductility factors under double impulse

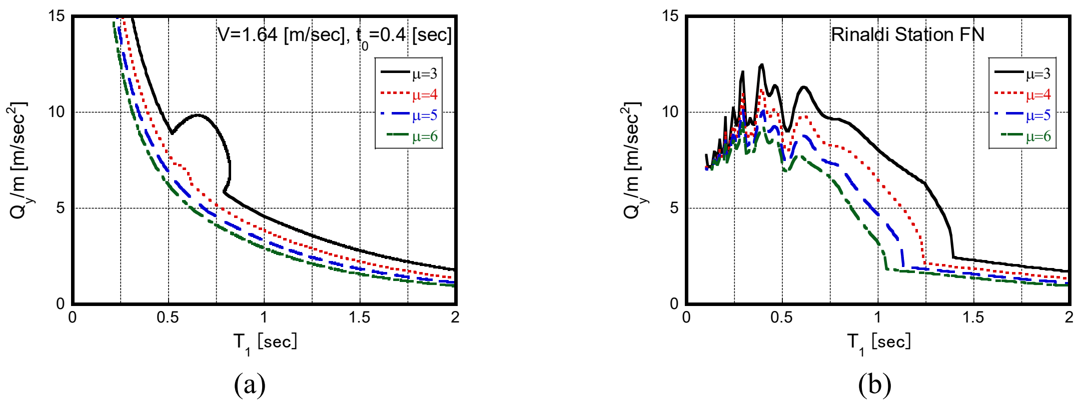

Fig. 15 – Elastic-plastic response spectrum for double impulse and Rinaldi Station FN: (a) Corresponding double impulse with V = 1.64 [m/sec] and t_0 = 0.4 [sec], (b) Main part of Rinaldi Station FN component

6. Conclusion

The double and multiple impulses were introduced for substituting the pulse-like ground motions and the long-duration ground motions, and the critical and non-critical inelastic responses subjected to those impulse inputs were derived in closed form. The conclusions may be summarized as follows.

(1) The closed-form expression for the maximum inelastic responses of an undamped elastic-perfectly plastic SDOF system under the critical double impulse input maximizing the response can be obtained by an energy approach. The critical timing is characterized as the time when the restoring force attains zero. Alternatively, the maximum inelastic responses to non-critical double impulse can be derived in closed form by the free vibration expression after the first impulse and the energy balance law.

(2) The closed-form expression for the steady-state inelastic response amplitudes of an undamped elastic-perfectly plastic SDOF system subjected to the critical multiple impulse input can be obtained by the energy balance law. The critical timing of each impulse is characterized as the time when the restoring force attains zero. In contrast, the plastic deformation subjected to non-critical multiple impulse input can be derived by using inelastic free-vibration responses after each impulse and the energy balance law. Although it is difficult to derive the plastic deformation directly as a function of the velocity amplitude and the time interval, the relation between the plastic deformation and the time interval can be obtained in closed form.

(3) An approximate elastic-plastic response spectrum for a pulse-like near-fault ground motion can be obtained analytically from the closed-form expression of the maximum inelastic responses to the critical and non-critical double impulse input. The proposed inelastic response spectrum can provide simple evaluation of the maximum elastic-plastic responses subjected to the pulse-type ground motion within reasonable accuracy.

7. References

[1] Kojima, K, and Takewaki, I: Critical earthquake response of elastic-plastic structures under near-fault ground motions (Part 1: fling-step input), *Frontiers in Built Environment*, 1: 12, 2015.

[2] Kojima, K, and Takewaki, I: Critical input and response of elastic-plastic structures under long-duration earthquake ground motions, *Frontiers in Built Environment*, 1: 15, 2015.

[3] Mavroeidis, G.P., and Papageorgiou, A.S.: A mathematical representation of near-fault ground motions, *Bull Seism Soc Am*, 93(3), 1099-1131, 2003.

[4] Sasani, M., and Bertero, V.V.: Importance of severe pulse-type ground motions in performance-based engineering: historical and critical review, in *Proc of the Twelfth World Conference on Earthquake Engineering*, Auckland, New Zealand, 2000.

[5] Takewaki, I., Murakami, S., Fujita, K., Yoshitomi, S., and Tsuji, M.: The 2011 off the Pacific coast of Tohoku earthquake and response of high-rise buildings under long-period ground motions, *Soil Dyn Earthq Eng*, 31, 1511-1528, 2011.

[6] Takewaki, I., and Tsujimoto, H.: Scaling of design earthquake ground motions for tall buildings based on drift and input energy demands. *Earthq Struct*, 2, 171-187, 2011.

[7] Caughey, T.K.: Sinusoidal excitation of a system with bilinear hysteresis, *J. Appl. Mech.*, 27(4), 640-643, 1960.

[8] Iwan, W.D.: The dynamic response of the one-degree-of-freedom bilinear hysteretic system, P*roceedings of the Third World Conference on Earthquake Engineering*, 1965.

[9] Kojima, K., Saotome, Y., Takewaki, I.: Critical earthquake response of a SDOF elastic-perfectly plastic model with viscous damping under double impulse as a substitute for near-fault ground motion. *Jpn Archit Rev*; 1: 207–220, 2018.

[10] Kojima, K., and Takewaki, I.: Critical Steady-State Response of Single-Degree-of-Freedom Bilinear Hysteretic System under Multi Impulse as Substitute of Long-Duration Ground Motion, *Frontiers in Built Environment*, 3: 41, 2017.

[11] Kojima, K., and Takewaki, I.: Closed-form critical earthquake response of elastic-plastic structures on compliant ground under near-fault ground motions, *Frontiers in Built Environment*, 2: 1, 2016.

